Cytogenet Genome Res 109:70–78 (2005)
DOI: 10.1159/000082384

Cytogenetic and Genome Research

# 3D Analysis of chromosome architecture: advantages and limitations with SEM

G. Wanner, E. Schroeder-Reiter and H. Formanek

Department of Biology I, Ludwig-Maximillians-Universität München, Munich (Germany)

Abstract. Three-dimensional mitotic plant chromosome architecture can be investigated with the highest resolution with scanning electron microscopy compared to other microscopic techniques at present. Specific chromatin staining techniques making use of simultaneous detection of back-scattered electrons and secondary electrons have provided conclusive information on the distribution of DNA and protein in barley chromosomes through mitosis. Applied to investigate the structural effects of different preparative procedures, these techniques were the groundwork for the "dynamic matrix model" for chromosome condensation, which postulates an energy-dependent process of looping and bunching of chromatin coupled with attachment to a dynamic matrix of associated protein fibers. Data from SEM analysis shows basic higher order chromatin structures: chromomeres and matrix fibers. Visualization of nanogold-labeled phosphorylated histone H3 (ser10) with high resolution on chromomeres shows that functional modifications of chromatin can be located on structural elements in a 3D context.



Investigation of three-dimensional (3D) chromosome architecture is a field of increasing significance, not only in terms of long-standing discussion of higher order chromosome structure but also in current efforts to understand nuclear functions in a 3D context. A variety of microscopic techniques, each with its own specific advantages and limitations, is available for 3D analysis of chromosomes: confocal laser scanning microscopy (CLSM), 3D reconstruction of serial ultrathin sections with the transmission electron microscope (TEM), stereo imaging of semi-thin sections (0.5–1 μm) with high voltage TEM (1 MeV), topographic imaging with the atomic force microscope (AFM) and topographic and stereo imaging with the scanning electron microsope (SEM). CLSM is extremely useful for in situ investigation of chromosomes, but is limited to use with fluorescent dyes, and by a resolution of approximately 250 nm. Although serial section reconstruction with TEM allows high resolution in the range of a few nanometers, it is prohibitively time consuming for routine analysis (Borland et al., 1988). Similarly, stereo imaging with high voltage TEM is limited to the thickness (1 μm) of sections (Ris, 1981). AFM can be performed on dry and even hydrated chromosomes; the resolution, however, is limited by the geometry of the scanning tip and elasticity of the chromosomes and can be achieved only in the order of 50–100 nm (Schaper et al., 2000). Topographic and stereo imaging with SEM allows the highest resolution (down to 5–10 nm) for 3D structural investigation of intact isolated chromosomes (Harrison et al., 1982; Allen et al., 1986; Sumner, 1991; Wanner and Formanek, 1995, 2000; Martin et al., 1996; Inaga et al., 2000b).

Over the past decade, preparation techniques for plant chromosomes, i.e. laser-marked slides, "drop/cryo" and "suspension" preparations, have been optimized for routine chromosome SEM investigation (Schubert et al., 1993; Martin et al., 1994). A variety of analytical techniques can be implemented, even three dimensionally by generating stereo images, by monitoring signals from secondary electrons (SE) and back-scattered electrons (BSE). DNA can be visualized separately after specific staining with either "platinum blue", a metal organic compound which reacts stoichiometrically with nucleobases (Wanner and Formanek, 1995), or with zirconium chloridoxide, which reacts with the phosphate backbone of DNA (Jander and

Supported in part by a grant from the German Research Council (Deutsche Forschungsgemeinschaft).

Received 20 August 2003; manuscript accepted 31 October 2003.

Request reprints from Gerhard Wanner, Department of Biology I
Ludwig-Maximillians-Universität München
Menzinger Strasse 67, DE–80638 Munich (Germany)
telephone: +49 (0)89 17861-237; fax: +49 (0)89 17861-248
e-mail: wanner@botanik.biologie.uni-muenchen.de

KARGER

Fax + 41 61 306 12 34
E-mail karger@karger.ch
www.karger.com



0301–0171/05/1093–0070$22.00/0

Accessible online at:
www.karger.com/cgr

Wendt, 1960; Wanner and Formanek, 2000). Proteins as a substance class can be localized with silver nitrate or silver colloids (Wanner and Formanek, 2000). Detection of specific proteins is possible with nanogold-labeled antibodies (Schroeder-Reiter et al., 2003). These analytic capabilities with SEM were the basis for the investigation of 3D chromosome structure and composition during the cell cycle and consequently for a structural chromosome model, the "dynamic matrix model" (Wanner and Formanek, 2000).

The aim of the present study was to obtain further structural information from mitotic plant chromosomes in different stages of condensation to contribute to the understanding of chromosome 3D ultrastructure. The influence of different preparative reagents on the structure of barley mitotic metaphase chromosomes was examined, with the intention of optimizing structural preservation for routine 3D analysis, and was used for acquiring insight into chromosome architecture. Specific staining and immunolabeling were applied to visualize protein(s) and DNA at various mitotic stages.

## Materials and methods

*Chromosome isolation*

Barley chromosomes were isolated and mounted either on laser marked glass slides (Laser Marking, Fischen, Germany) with the "drop/cryo" technique (Martin et al., 1994) or on standard glass with the "suspension" technique (Schubert et al., 1993). Chromosome control slides were subsequently fixed in 2.5% glutaraldehyde or 2% formaldehyde in cacodylate buffer (75 mM, pH 7). Slides for immunolabeling were incubated in phosphate-buffered solution (PBS, 0.13 M NaCl, 7 mM $Na_2HPO_4$, 3 mM $NaH_2PO_4$, pH 7.0 with 0.1% Tween 20).

*Cryo fracture technique*

Cryo fracture of barley root tips was performed according to Tanaka (1980) modified by replacing dimethylsulfoxide with dimethylformamide and omitting osmium tetroxide thiocarbohydrazide impregnation cycles. For detection of DNA, root tips were stained according to Wanner and Formanek (1995) with platinum blue, an oligomer of bis(acetonitrile)-platinum $[(CH_3CN)_2Pt]_n$, for 1 h after glutaraldehyde fixation.

*Controlled decondensation*

In controlled decondensation experiments the following buffers and reagents were used at room temperature: i) citrate buffer (60 mM Na citrate, 15 mM $CaCl_2$, pH 7.2) for 60 min; ii) Tris/HCl buffer (10 mM, pH 7.2), iii) 1% dextran sulfate in distilled water (MW 700,000, ICN Biomedicals); iv) cacodylate buffer (75 mM, pH 7). For proteinase K treatment chromosomes were first fixed with glutaraldehyde (2.5% in 75 mM cacodylate buffer) and then treated with proteinase K (1 mg/ml, ICN Biochemicals) for 2 h at 37°C.

*DNA and protein staining*

For separate visualization of DNA, chromosomes were stained for 30 min at room temperature with platinum blue (10 mM, pH 7.2; Wanner and Formanek, 1995). DNase treatment (50 µg/ml in distilled water, 2 h at 30°C) was performed prior to glutaraldehyde fixation. Proteins were separately visualized after staining for 12 h at 60°C with 20% aqueous silver nitrate solution or with an aqueous solution of colloidal silver (0.5 g silver nitrate dissolved in 1.5 ml water gradually added to 25 ml of an aqueous solution of 0.25% tannic acid and 2% sodium carbonate) containing 0.1 M of elementary silver at pH 8, as described in detail in Wanner and Formanek (2000).

*Immunolabeling*

Immunolabeling was performed according to Schroeder-Reiter et al. (2003), with the primary polyclonal rabbit antibody against histone H3 phosphorylated at serine position 10 (Upstate Biotechnologies, NY, USA), secondary anti-rabbit Fab′ fragment labeled with Nanogold® (Nanoprobes, NY, USA), and silver-enhanced according to manufacturer's instructions (HQ Silver™ enhancer kit, Nanoprobes) (For review of nanogold labeling and enhancement procedure see Hainfeld et al., 1999; Hainfeld and Powell, 2000).

*SEM*

After a final wash in distilled water; the slides were washed in 100% acetone (for IM preparations) or graded acetone series (20–100%), critical point dried and located on laser-marked slides (for easier searching and comparison in SEM) with LM in phase contrast mode. Preparations exclusively examined in the secondary electron (SE) mode were sputter-coated with platinum; preparations for backscattered electron (BSE) detection (stained and immunolabeled specimens) were carbon-coated by evaporation (in both cases to a layer of 3–5 nm with a Magnetron SCD 050, Balzers, Liechtenstein) and examined at an accelerating voltage of 8 kV (exclusively for SE images) or 12–30 kV (for simultaneous SE and BSE imaging) with a Hitachi S-4100 field emission scanning electron microscope equipped with a YAG-type BSE-detector (Autrata). SE and BSE images were recorded simultaneously with Digiscan™ hardware and processed with Digital Micrograph 3.4.4 software (Gatan, Inc., Pleasantdon, CA, USA). Element analysis by energy dispersive X-ray analysis (EDX) was performed with a Noran "Vantage" system equipped with a light element silicon detector (Pioneer) and an ultra-thin window.

## Results and discussion

*Imaging of chromosomes in situ*

Ideally chromosomes should be investigated in situ after optimal fixation. To this end, the well established Tanaka cryo fracture technique (Tanaka, 1980) was applied to barley root tips for visualization with scanning electron microscopy (SEM). However, in spite of a variety of modifications of the method, 3D visualization of chromosomes was not conclusive. Both nucleoplasm and cytoplasm, particularly in meristematic cells, appear extremely compact and prohibit a three dimensional view of chromosomes (Fig. 1). The chromosomes themselves are also compact units, which appear homogeneous even when fractured. When root tips are stained with platinum blue for DNA, chromosomes can be distinguished from the nucleoplasm in all stages of condensation (Fig. 1). However, because of the 3D distribution in the nucleus, the substructure of individual chromosomes cannot be determined. Although this technique has been successfully applied for certain specific topics (Inaga et al., 2000a), in general it is not yet routinely applicable for structural investigations of mitotic metaphase chromosomes.

*Structural changes during chromosome preparation*

The classical "drop" technique for isolating chromosome metaphase spreads, established for use in light microscopy (LM), seems to be an ideal alternative for SEM, but has proven to be difficult mainly for two reasons: frequently artificial surface layers form during drying which obscure chromosome details (Allen et al., 1988; Sumner, 1996) and chromosomes tend to flatten. In principle, 3:1 ethanol:acetic acid fixation, which has been successfully applied for the last century for LM investigations, is problematic for high resolution SEM studies because of its denaturing and dehydrating properties which lead to inadequate chromosome structure, especially when air-

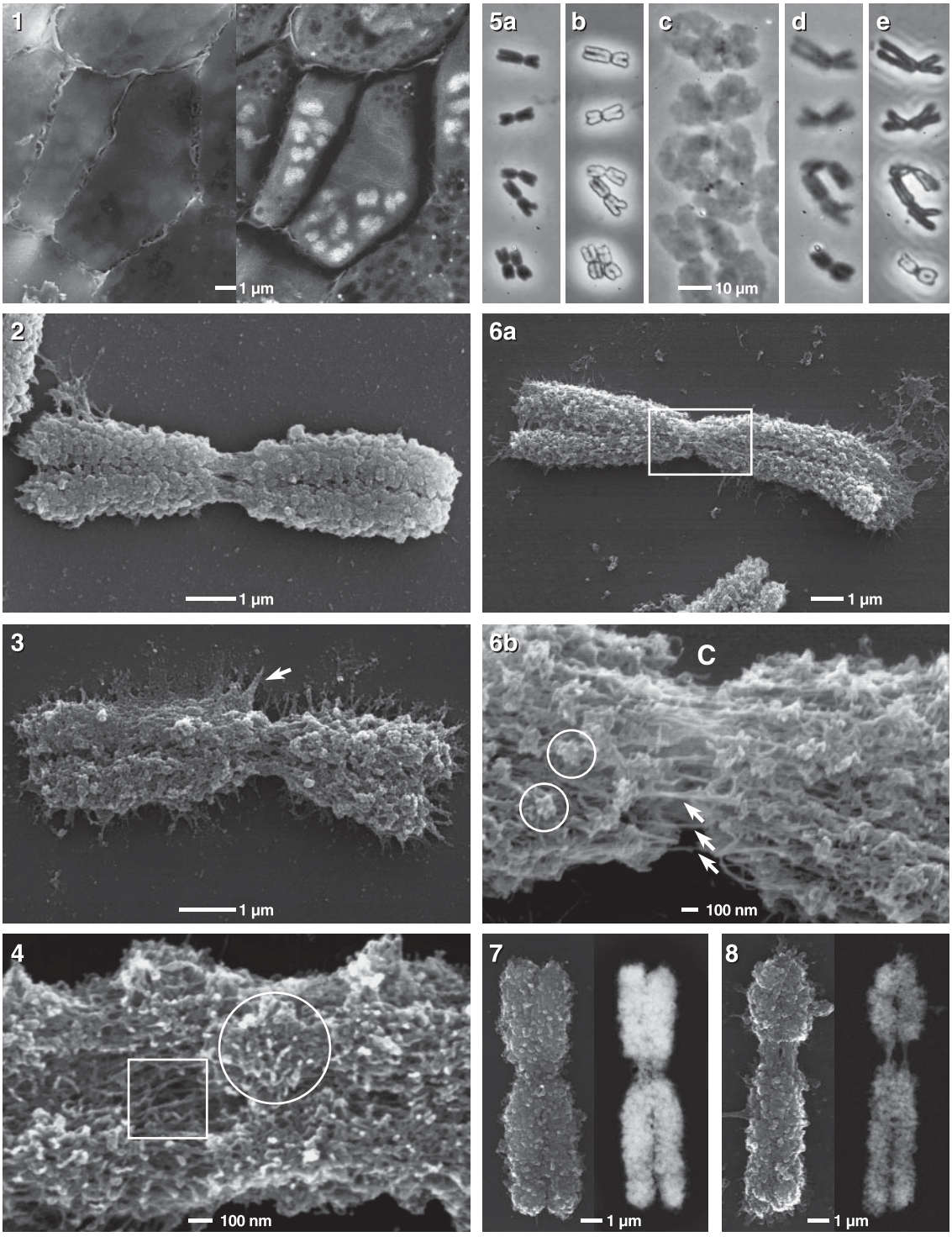


Fig. 1. Scanning electron micrograph of a cryo fracture of a barley root tip stained for DNA with platinum blue. During metaphase, both cytoplasm and nucleoplasm are so dense that a three-dimensional insight is not posssible in the SE image (left). BSE image allows recognition of prometaphase chromosomes by the bright signals (right).

Fig. 2. Scanning electron micrograph of a barley metaphase chromosome, fixed with 3:1, and spread according the drop/cryo technique. The centromere and the two chromatids, which are partly separated, are clearly visible. The dominant substructure of the chromatids, at this low magnification level, are "knobby" chromomeres and a centromere with parallel fibers.

Fig. 3. Scanning electron micrograph of a barley metaphase chromosome from a chromosome suspension (fixed with formaldehyde and spread by cyto-spin centrifugation). Chromosome ultrastructure is similar to the drop/cryo technique, with the difference that the chromatin (chromomeres) is somewhat loosened and chromatin "stress fibers" have developed (arrow).

Fig. 4. Scanning electron micrograph of a barley prophase chromosome (detail). Highly condensed regions composed of chromomeres (circle) are interspersed with chromatin domains with a parallel arrangement of fibers (square).

dried. Establishing the drop/cryo technique eliminated an air-drying step, allowing routine isolation of accessible and well-preserved chromosomes (Fig. 2). Since chromosomes are frozen after fixation and directly transferred into buffered glutaraldehyde, chromosomal proteins are fixed in a fully rehydrated state. However, in further preparation stages for SEM minor changes in size resulting from dehydration and from critical point drying (CPD) are observed.

For comparison, we applied alternative fixation methods omitting 3:1 fixation, using only glutaraldehyde or formaldehyde. Glutaraldehyde fixes root tips so efficiently, that chromosomes cannot be isolated from nucleoplasm/cytoplasm. However, chromosomes can be liberated from fixed large pollen mother cells of *Lilium longiflorum* by gently squeezing, revealing a loosened chromatin structure. Suspension chromosomes isolated from root tips fixed with formaldehyde do not maintain their orientation in metaphase spreads and are not as well ultrastructurally preserved compared to drop/cryo preparations (Fig. 3). Frequently we observed in both LM and SEM stretching in the centromeric region, which is probably caused by centrifugal force from the cytospin centrifugation of chromosomes onto the slides (even with very low 400 rpm), and/or "stress fibers" (Fig. 3). When comparing chromatin substructure to drop/cryo chromosomes, suspension chromosomes are generally less compact (Fig. 3, compare with Fig. 2).

*Structural elements of mitotic plant chromosomes*

Investigation of a variety of plants revealed that basic chromosome substructures are more or less universal. Chromosomes – throughout all stages of the cell cyle – are composed of fibrous structures which vary in diameter and orientation. The predominant fibers observed have a diameter of approximately 30 nm (Martin et al., 1996). Some of these fibers are "bunched", forming chromomeres with diameters ranging from 200 to 400 nm (Fig. 4). During condensation from prophase to prometaphase, chromomeres are interspersed with chromatin domains with a parallel arrangement of fibers which are defined as parallel matrix fibers (Fig. 4). Basically, mitotic metaphase chromosomes show two characteristic features: two attached more or less cylindrical sister chromatids which appear "knobby" at low magnifications due to tightly packed chromomeres, and a centromeric region seen as a constriction with characteristic parallel fibers (Fig. 2). Secondary constrictions are characterized, like the centromere, by parallel matrix fibers. In the case of *Luzula sylvatica* (wood rush) which has polycentric chromosomes showing no centromeric constriction in LM, SEM investigations confirmed lack of constriction and showed parallel fibers exposed interspersedly with chromomeres along the entire chromosome (data not shown).

*Chromosome condensation and decondensation*

Condensation of barley chromosomes in mitosis starts in the centromeric region and then continues toward telomeres (Martin et al., 1996). During further condensation from prophase to prometaphase, chromomeres are interspersed with parallel matrix fibers (Fig. 4). The number of chromomeres increases with further condensation, with higher density of packing towards the centromere. At maximum condensation – and typically for arrested chromosomes – chromomeres are so tightly compacted that the chromosome surface appears rather homogeneous. It should be noted that, according to our observations, arresting has a significant influence on chromosome morphology: in general it causes an (artificial) shortening and consequently a compaction of the chromosomes with much more pronounced constrictions. This could be explained as follows: an antiparallel movement of the matrix fibers, as described by the dynamic matrix model, is an energy-dependent process which is limited sterically in binding sites, and which is counteracted by elastic tension (potential energy) in the condensed chromomeres. Under normal conditions these two forces reach an equilibrium, which can be shifted depending on preparative treatment (in this case interruption of spindle apparatus formation).

Decondensation in telophase starts at the telomeres followed by successive disappearance of the distinct shape of the chromosomes. When examined at high magnification, chromomeres become again discernible, typically arranged in clusters but subsequently separating and unraveling as decondensation progresses. Matrix fibers can still be observed, but are no longer in parallel arrangement. In physical terms, decondensation of chromosomes could be described as a release of potential energy in the chromomeres and matrix fibers.

*Chromosomes as a "loaded spring"*

By fixation of the chromosomes (3:1, glutaraldehyde, formaldehyde) not only structural elements but also the potential energy are preserved. This can be demonstrated by several experimental applications which cause the chromosomes to spread. Chromosomes fixed only in 3:1 are very sensitive to changes in buffer milieu (i.e. Tris, citrate buffer, PBS buffer,

Fig. 5. Light micrographs of a barley metaphase spread illustrating the high structural flexibility of chromatin after fixation and treatment with proteinase K. Chromosomes were first fixed with 3:1, spread according to the drop/cryo technique, then fixed with 2.5% glutaraldehyde (a) and subsequently incubated with proteinase K (b–c). After 30 min at RT chromosomes swell, which inverts contrast in phaco (b). After 2 h at 37 °C, chromosomes spread dramatically in length and width (c). Surprisingly, after washing and dehydration with acetone they recover to a large degree in size and shape, but still differ from the initial dimensions: chromosomes are longer; chromosome arms lie at different angles; chromatids are more separated (d). After critical point drying there do not appear to be any significant structural changes; the contrast however is different, as the specimen is photographed in a dry state without cover slip, and minor shrinkage can be observed (e).

Fig. 6. Scanning electron micrograph of a barley metaphase chromosome, first fixed with 3:1, spread according to the drop/cryo technique, then incubated with 1% dextran sulphate for 5 min. Chromosomes stretch about 30% (a) with loosening of the individual chromomeres (b) (circles). In the centromeric region (C) parallel matrix fibers are exposed (b) (arrows).

Figs. 7, 8. Scanning electron micrographs of a barley metaphase chromosome stained for DNA with platinum blue. The conventional SE image (7, left) shows both DNA and protein, whereas the BSE signal (7, right) monitors DNA content, which is high in areas corresponding with the "knobby" chromomeres and lower in the centromeric region and between the sister chromatids. If chromosomes are treated with DNaseI before glutaraldehyde fixation and DNA staining (8), the BSE signal is reduced in intensity (8, right) without a corresponding change in the global chromosome structure as evident from the SE-image (8, left). Note the significant discrepancy between topographic information and DNA distribution in the centromeric region.

cacodylate buffer). In principle, every change in milieu, even in relevant physiological concentrations, may change chromosome structure significantly, and can in some cases even be observed in LM (Fig. 5). Typical structural changes which occur are a) flattening, b) loosening, c) stretching d) spreading, or a combination thereof. For example, dextran sulfate (commonly used for in situ hybridisation) causes lengthening of the chromosomes and loosening of the chromomeres (Fig. 6a, b). Structural changes may occur over the entire chromosome or are limited to certain regions (ie. centromere, telomere, chromosome arms). In all cases studied, the stretching of the chromosomes results in separation of the otherwise densely packed chromomeres, revealing matrix fibers within the chromosome arms (Fig. 6b). Chromosomes fixed in 3:1 and subsequently in formaldehyde or glutaraldehyde are more stable with regard to buffers and preparative reagents, but are still subject to structural changes.

On glutaraldehyde-fixed chromosomes, visualizing DNA by staining with platinum blue reveals that DNA is not evenly distributed along the chromosome: constrictions at the centromeric and the satellite regions contain less DNA than other regions (Fig. 7). Because of their high DNA content, chromomeres are also discernible in the BSE image (Fig. 7). Chromosomes treated with DNaseI (before glutaraldehyde fixation) and subsequently stained with platinum blue show a significantly weaker BSE signal, but remain structurally surprisingly intact (Fig. 8), implying that non-DNA/protein components are largely responsible for the integrity of chromosome structure. Superposition of BSE and SE images facilitates comparison of structure and composition (Figs. 9–16), and, especially at higher magnification, shows that chromosome arms stain intensely for DNA (Fig. 9), whereas the centromeric constriction, characterized structurally by exposed parallel matrix fibers, hardly stains for DNA at all (Fig. 10). Energy-dispersive X-ray analysis (EDX) confirmed that the BSE signal arose from platinum. Staining with silver compounds enables recognition of proteins: The tannic acid shell of colloidal silver reacts with chromosomal proteins, as does silver nitrate, albeit preferentially in centromeric and telomeric regions. Although silver staining tends to produce weaker signals than platinum blue staining for DNA – not only due to the lower atomic number ($^{47}$Ag) compared to platinum ($^{78}$Pt) but also possibly due to instability of silver compounds and, in the case of colloidal silver, to sterical accessibility into chromatin – both silver stains clearly indicate that the exposed parallel matrix fibers in the centromere are protein enriched (Fig. 11).

Influence of buffers, primarily investigated to monitor artificial structural changes, proved to be useful in simulating decondensation and, in combination with SEM analytic techniques, providing insight into internal chromosome structure and composition. Chromosomes incubated in citrate buffer typically are somewhat stretched and "fan out" in all four telomeres giving the chromosome an X-shape; the centromeric region remains relatively unaffected and stains intensely for DNA, but the "fanned out" telomeric regions reveal underlying non-DNA structural elements (Fig. 12).

In general, the stronger the fixation, the less influence of subsequent treatment with buffers or detergents. Glutaraldehyde, however, fixes proteins so well that the 3D structure is unaffected by most reagents. We postulate that potential energy (formed during condensation) is thus best conserved in metaphase chromosomes. Unfixed chromosomes are digested within minutes even at very low concentrations of proteinase K (0.1–1 μg/ml), whereas fixed chromosomes remain unaffected. Surprisingly however, if fixed chromosomes are treated with a 100- to 1000-fold concentration of proteinase K (0.1–1.0 mg/ml), a minor fraction of the fixed proteins is digested. This has a dramatic (time-dependent) effect on the chromosomes: they stretch in length and/or fan out in breadth. This artificial loosening of the compact metaphase chromosomes is referred to as "controlled decondensation" (Wanner and Formanek, 2000).

In contrast to buffer influences, controlled decondensation in barley chromosomes typically starts in the centromere, and then extends in a linear fashion over the entire chromosome. In some cases, chromosomes reached an extraordinary length of up to 200 μm. DNA staining of proteinase K-treated chromosomes reveals a loosened chromomere configuration, with interspersed and underlying non-DNA matrix fibers (Figs. 13 and 14). Indeed, consistent with all cases of stretching or loosening of chromosomes, parallel matrix fibers can be observed over the total length of the chromosome. In the extreme stage of (controlled) decondensation, chromatin begins to stretch to elementary chromatin substructures: "bunched" solenoids (chromomeres, on average 200 nm), solenoids (30 nm) and elementary fibers (10 nm). DNA staining of stretched chromosomes reveals that i) the strongest BSE signal correlates with chromomeres; ii) there are fibers which stain for DNA; iii) there are fibers which do not stain for DNA. Since protein matrix fibers and DNA solenoids are in the same range of size (30 nm) they cannot be distinguished solely on the base of structural characteristics. Controlled decondensation can be interpreted according to the dynamic matrix model as follows: Since chromatin and protein matrix fibers are associated tightly by loop binding and matrix binding proteins, even partial digestion of these proteins releases tension created by chromatin compaction, causing the observed stretching and spreading.

Figs. 9, 10. DNA distribution in a barley metaphase chromosome stained for DNA with platinum blue. For better visualization, the signals of SE (yellow) and BSE (blue) are superimposed. Typical for metaphase chromosomes is a weaker BSE signal in the centromeric region (9; see also Fig. 7). If chromosomes are treated with proteinase K, chromosomes stretch first in the centromeric region which gives a better insight into chromatin substructures. Higher magnification reveals that the centromeric region is DNA depleted: the BSE signal (blue) fades out and that the exposed matrix fibers exhibit mainly SE signal (yellow) (10).

Fig. 11. Protein distribution in a barley metaphase chromosome stained with silver nitrate. Signals of SE (yellow) and BSE (red) are superimposed. Silver nitrate reacts with chromatin, preferentially however in the centromeres (C) and the telomeres. BSE signal shows that the centromere is protein-enriched.

Fig. 12. Scanning electron micrograph of barley metaphase chromosomes after controlled decondensation with citrate buffer and staining with platinum blue for DNA. Signals of SE (yellow) and BSE (blue) are superimposed. Chomosomes decondense, most pronouncedly at the telomeres. During flattening, the DNA-rich (blue) chromomeres separate and a protein-rich network of matrix fibers (yellow) becomes visible.

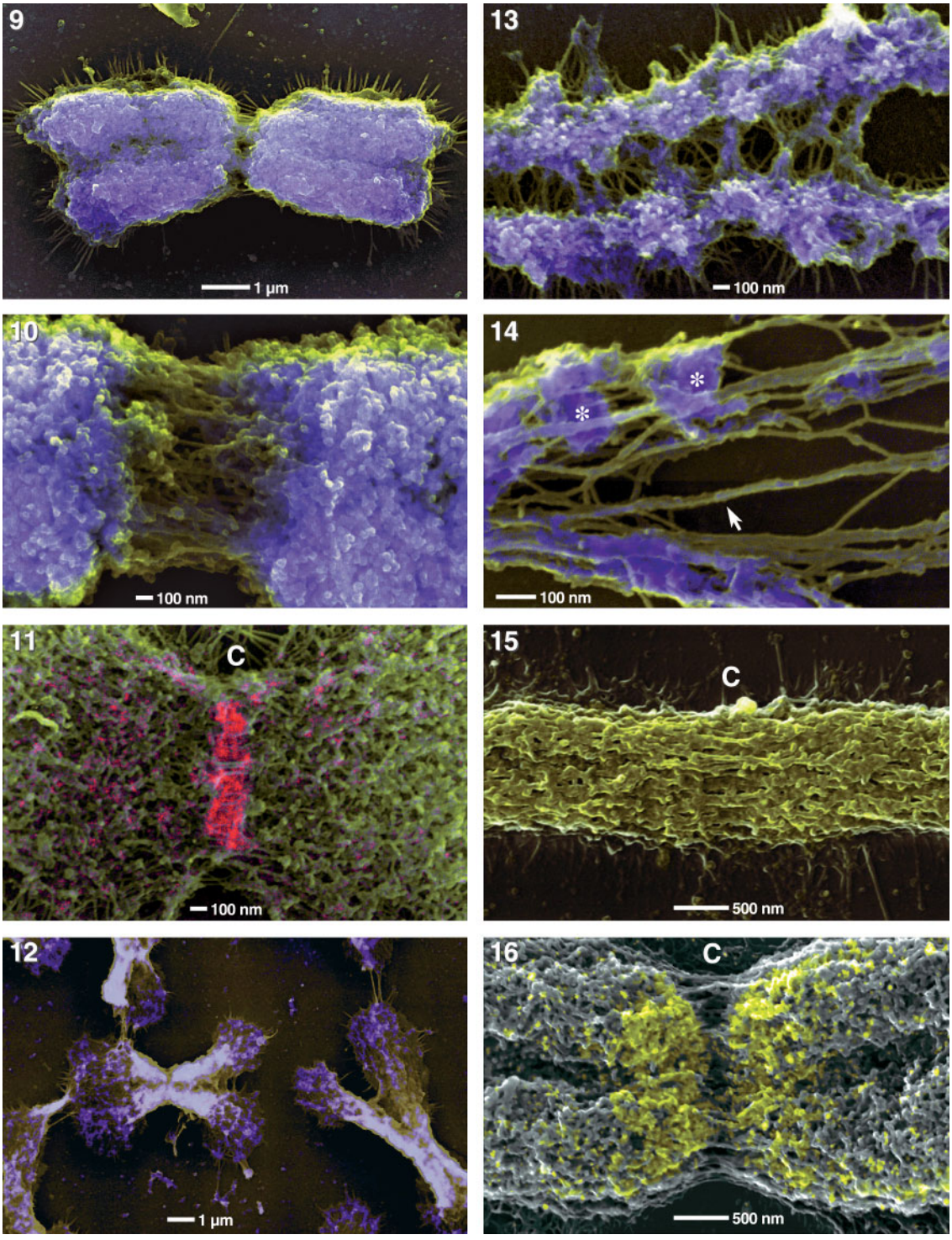


Fig. 13. Scanning electron micrograph of a barley prophase chromosome (detail) after fixation with glutaraldehyde, subsequent controlled decondensation with proteinase K and staining with platinum blue for DNA. Signals of SE (green) and BSE (purple) are superimposed. Sister chromatids, which are predominantly composed of chromomeres and matrix fibers, stretch and separate. Chromomeres exhibit high DNA content (purple), whereas matrix fibers (green) – which show only a neglegible DNA signal – become exposed and lose their parallel orientation.

Fig. 14. Scanning electron micrograph of a barley metaphase chromosome (detail) after fixation with glutaraldehyde, subsequent controlled decondensation with proteinase K and staining with platinum blue for DNA. Signals of SE (green) and BSE (blue) are superimposed. The chromosomes are stretched nearly to a maximum: chromomeres are widely separated, and some are stretched , loosened or "unraveled", but still show an intense DNA signal (purple; asterisks). The matrix fibers show either no, or a very weak, BSE signal (arrow).

Figs. 15, 16. Scanning electron micrographs of barley pro-metaphase and metaphase chromosomes labeled for phosphorylated histone H3. BSE image of signal (green) is superimposed onto the grey-scale topographic SE image. In pro-metaphase (15) there is an even signal distribution over the centromere which is characterized by parallel matrix fibers but not by a constriction. In metaphase (16) the parallel matrix fibers at the centromere (C) are exposed in a narrow region which is coincident with the signal gap.

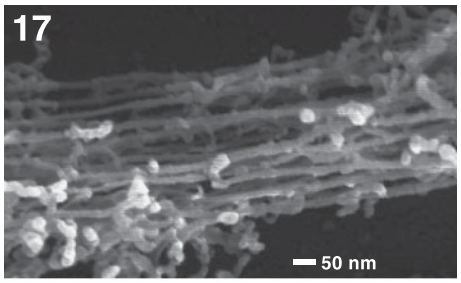


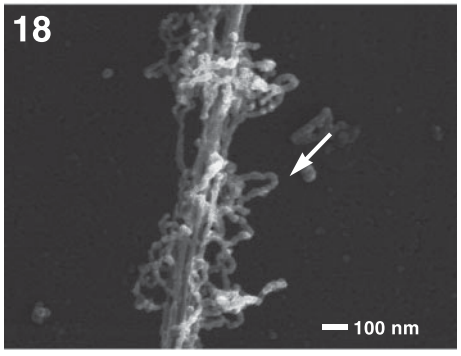


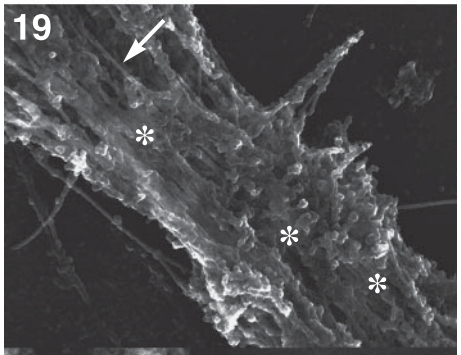


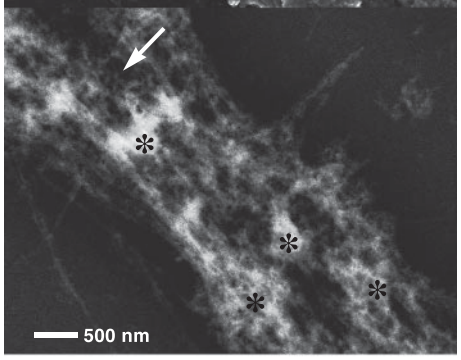


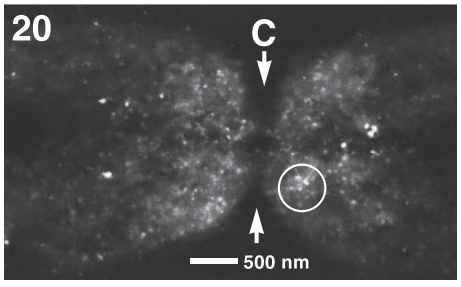


Figs. 17, 18. Stereomicrographs of barley metaphase chromosomes after fixation with glutaraldehyde and treatment with proteinase K at different stages of decondensation. During stretching, the architecture of the centromere becomes visible: it is predominantly composed of parallel matrix fibers (17). Further stretching reveals that the entire chromosome arms consist of both parallel matrix fibers and chromomeres. After ultimate stretching, the number of matrix fibers is decreased and the chromomeres are stretched and decondensed to the level of the solenoid loops (arrow).

Fig. 19. Pair of stereomicrographs of barley metaphase chromosomes fixed first with glutaraldehyde, then treated with proteinase K for controlled decondensation and stained for DNA distribution with platinum blue (upper stereo-pair: SE Signal of DNA + protein; lower stereo-pair: BSE signal from DNA). Some matrix fibers are not stained (arrow). The DNA is distributed mainly in a network, with the highest concentration in chromomeres (asterisks).

Fig. 20. Stereo micrographs of barley chromosomes in metaphase labeled for phosphorylated histone H3 (ser10). The BSE stereo pairs provides three dimensional depth information. Signals can be observed from different planes within the chromosome, facilitating recognition of individual signal spots, especially in regions of high signal density (circle). Although parallel matrix fibers at the centromere (C) are exposed from pro-metaphase to metaphase (see Figs. 15 and 16), the signal gap is exclusive to late metaphase (arrows).

Gold-labeled phosphorylated histone H3 at serine 10 (H3P) could be directly associated with corresponding chromosomal structure(s) detected simultaneously by BSE and SE. A change in H3P distribution on barley chromosomes during mitosis, documented in LM studies (Houben et al., 1999; Manzanero et al., 2002), could be confirmed with indirect immunogold labeling and SEM analysis, revealing a correlation between increasing compaction of chromomeres and increasing signal intensity in the pericentric region. Up to prometaphase, at which stage the chromomeres are still loose and the centromeric constriction is not yet pronounced, H3P signals are evenly distributed on the chromosome (Fig. 15). At metaphase, the majority of labeled H3P is found on the highly condensed chromomeres bordering the centromere. Parallel fibers, visible at metaphase in the centromere, are not labeled (Fig. 16).

*3D Imaging*

Interpretation of a 3D structure is limited when evaluating topographic (2D) images. Stereo micrographs of SE and BSE signals allow visualization of chromosomes in true three dimensions. In the case of controlled-decondensed chromosomes, stereo SE images allow insight into loosened chromomeres and precise orientation of parallel matrix fibrers, which are obviously under tension. During stretching, the 3D orientation of the predominant parallel matrix fibers in the centromere is striking (Fig. 17). Stretching causes chromomeres to linearly separate, exposing an increasing number of parallel matrix fibers. Further stretching reveals that the entire chromosome arms consist of both matrix fibers and chromomeres. After ultimate stretching the number of matrix fibers is decreased and the stretched chromomeres are decondensed to loops at the level of the solenoids (30-nm fibers) (Fig. 18). Comparison of SE and BSE stereo images after proteinase K treatment and platinum blue staining shows DNA-enriched areas (chromomeres in various stages of decondensation) and a fraction of fibers which, deduced from the BSE signal, contain no (or undetectable amounts) of DNA (parallel matrix fibers) (Fig. 19).

As BSEs from noble metals can be detected at 15 kV from a depth of 1–1.5 μm within an organic matrix, it is possible to

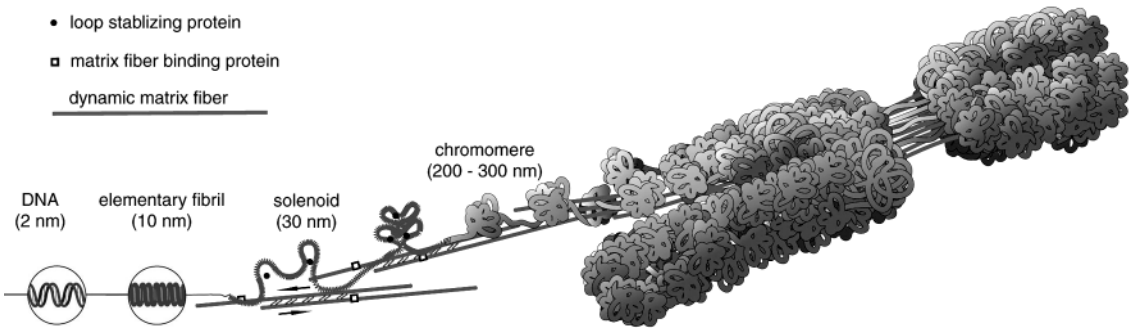


Fig. 21. Schematic drawing illustrating different levels of chromatin condensation according to the dynamic matrix model. DNA (2nm) assembles with histone proteins, forming nucleosomes and the elementary fibril (10 nm) which winds up to a solenoid (30 nm). Solenoids attach to polymerizing matrix fibers by matrix fiber binding proteins. Dynamic matrix fibers associate and move anti-parallel to each other (arrows). As condensation progresses, attached solenoid loops are "bunched" into chromomeres (200– 300 nm) which are stabilized by loop stabilizing proteins. During condensation chromosomes become shorter and thicker as more chromomeres are formed. This creates a tension perpendicular to the axial direction which forces the chromatids apart.

visualize a 3D signal distribution from within chromosomes, enabling more precise location of signals onto the chromatin in a 3D context. The more complex the labeling, the more sterical hindrance becomes a problem. However, stereo images of immunogold labeling of H3P clearly show that signals originate not only from the surface but also from within chromosomes (Fig. 20), indicating that chromomeres are distributed throughout the chromosome.

*Dynamic matrix model*

In summary, based on SEM analysis, basic structural elements, different degrees of condensation and the mechanisms of condensation can be accomodated by the dynamic matrix model (Fig. 21). Briefly, chromosomes are mainly composed of DNA packed in chromomeres and a dynamic matrix formed of parallel protein fibers. Chromosome condensation is achieved by binding of solenoids to matrix fibers which have reciprocal contact sites and move antiparallel to each other, causing loops of solenoids to accumulate to form additional chromomeres (Fig. 21). As condensation progresses, a tension perpendicular to the axial direction contributes to the forces involved in chromatid separation, giving metaphase barley chromosomes their typical shape. This correlates with most chromosome models – with the exception of helical coiling, which has never been observed in our studies – and with long-standing TEM and molecular evidence of a protein matrix (for review see Stack and Anderson, 2001).

*Outlook*

Preservation of 3D structure of chromosomes in combination with high resolution SEM and analytical methods remains an elusive goal, as "fixation" (Lat., to fasten) and "analysis" (Gr., loosening up) are a contradiction in terms. Since nearly every treatment of isolated chromosomes causes structural changes, an adequate fixation is unavoidable, which in turn inhibits access to analytical reagents, particularly in the case of immunodetection.

Despite this, efforts are being made on different fronts to optimize 3D investigations by increasing resolution. With modern equipment, high resolution structural investigations with SE detection of chromatin topography should already be possible at low voltage (1 kV) with an instrumental resolution of about 1 nm, thus requiring thinner metal coating (down to 1 nm) and enabling a routine significant improvement of specimen resolution down to 2–3 nm. This would allow for a more precise visualization of solenoids and elementary fibers.

For techniques using BSE detection, and especially for 3D visualization, use of plastic (carbon-based) slides for isolated chromosomes would eliminate BSE noise originating from glass (silicon) slides and increase the resolution of true BSE signals. However, a chromosome preparation technique must be newly established to accomodate spreading on (hydrophobic) carbon-based plastics, and is yet unresolved in our lab.

Labeling efficiency with immunogold also leaves room for improvement. Depending on the degree of chromosome fixation (i.e. accessibility for antibodies) and on the size of markers, localization of epitopes down to the solenoid level (30 nm) of chromatin is possible at present. Critical and essential for further investigations with increased sensitivity is the reduction of background by using alternative secondary antibodies and optimizing metallonucleo-enhancement. Development of direct labeling systems, preferentially with Fab′ fragments and 5–8 nm gold markers which could be detected without enhancement, would permit localization of markers even to the elementary fibril (10 nm). Identifying components or modifications of chromatin and locating them in a three dimensional context will contribute to further understanding of chromosome structure and function.

## Acknowledgements

The authors gratefully acknowledge excellent technical assistance from Sabine Steiner and artwork by Renate Reichinger-Bock. Micrographs from cryo fracture were kindly provided by Ursula Wengenroth.

## References


Allen TD, Jack EM, Harrison CJ, Claugher D: Scanning electron microscopy of human metaphase chromosomes. Scanning Electron Microsc 1:301–308 (1986).

Allen TD, Jack EM, Harrison CJ: The three-dimensional structure of human metaphase chromosomes determined by scanning electron microscopy, in Adolph KW (ed): Chromosomes and Chromatin, pp 51–72 (CRC Press, Boca Raton 1988).

Borland L, Harauz G, Gahr G, van Heel M: Packing of the 30 nm chromatin fiber in the human metaphase chromosome. Chromosoma 97:159–163 (1988).

Hainfeld JF, Powell RD: New frontiers in gold labeling. J Hist Cytochem 48:471–480 (2000).

Hainfeld JF, Powell RD, Stein JK, Hacker GW, Hauser-Kronberger C, Cheung ALM, Schöfer C: Gold-based autometallography, in: Proceedings of the Fifity-seventh Annual Meeting, Microscopy Society of America, pp 486–487 (Springer, New York 1999).

Harrison CJ, Allen TD, Britch M, Harris R: High-resolution scanning electron microscopy of human metaphase chromosomes. J Cell Sci 56:409–422 (1982).

Houben A, Wako T, Furushima-Shimogawara R, Presting G, Künzel G: The cell cycle dependent phosphorylation of histone H3 is correlated with the condensation of plant mitotic chromosomes. Plant J 18:675–679 (1999).

Inaga S, Naguro T, Kameie T, Iino A: Three-dimensional ultrastructure of *in situ* chromosomes and kinetochores of *Tradescantia reflexa* anther cells by scanning electron microscopy: 1. Freeze-cracked meiotic chromosomes and kinetochores in pollen mother cells. Chrom Sci 4:1–9 (2000a).

Inaga S, Naguro T, Kameie T, Iino A: Three-dimensional ultrastructure of *in situ* chromosomes and kinetochores of *Tradescantia reflexa* anther cells by scanning electron microscopy: 2. Whole mounted chromosomes and kinetochores of pollen mother cells and tapetal cells. Chrom Sci 4:11–20 (2000b).

Jander G, Wendt H: Lehrbuch der Analytischen und Präparative Anorganischen Chemie, p 129 (Hirzel, Leipzig 1960).

Manzanero S, Rutten T, Kotseruba V, Houben A: Alterations in the distribution of histone H3 phosphorylation in mitotic plant chromosomes in reponse to cold treatment and the protein phosphatase inhibitor cantharidin. Chromosome Res 10:467–476 (2002).

Martin R, Busch W, Herrmann RG, Wanner G: Efficient preparation of plant chromosomes for high-resolution scanning electron microscopy. Chromosome Res 2:411–415 (1994).

Martin R, Busch W, Herrmann RG, Wanner G: Changes in chromosomal ultrastructure during the cell cycle. Chromosome Res 4:288–294 (1996).

Ris H: Stereoscopic electron microscopy of chromosomes. Meth Cell Biol 22:153–170 (1981).

Schaper A, Rößle M, Formanek H, Jovin TM, Wanner G: Complementary visualization of mitotic barley chromatin by field-emission scanning electron microscopy and scanning force microscopy. J Struct Biol 129:17–29 (2000).

Schroeder-Reiter E, Houben A, Wanner G: Immunogold labeling of chromosomes for scanning electron microscopy: A closer look at phosphorylated histone H3 in mitotic metaphase chromosomes of *Hordeum vulgare*. Chromosome Res 11:585–596 (2003).

Schubert I, Dolezel J, Houben A, Scherthan H, Wanner G: Refined examination of plant metaphase chromosome structure at different levels made feasible by new isolation methods. Chromosoma 102:96–101 (1993).

Stack SM, Anderson LK: A model for chromosome structure during the mitotic and meiotic cell cycles. Chromosome Res 9:175–198 (2001).

Sumner AT: Scanning electron microscopy of mammalian chromosomes from prophase to telophase. Chromosoma 100:410–418 (1991).

Sumner AT: Problems in preparation of chromosomes for scanning electron microscopy to reveal morphology and to permit immunocytochemistry of sensitive antigens. Scanning Microscopy Suppl 10:165–176 (1996).

Tanaka K: Scanning electron microscopy of intracellular structures. Int Rev Cytol 68:97–125 (1980).

Wanner G, Formanek H: Imaging of DNA in human and plant chromosomes by high-resolution scanning electron microscopy. Chromosome Res 3:368–374 (1995).

Wanner G, Formanek H: A new chromosome model. J Struct Biol 132:147–161 (2000).